Theory of the anisotropic ferrite wake-field accelerator. II. Higher-order modes

Jintana T. Chiu and Sekazi K. Mtingwa
High Energy Physics Division, Argonne National Laboratory, Argonne, Illinois 60439
(Received 6 August 1990; revised manuscript received 26 December 1990)

The theory of the anisotropic ferrite wake-field accelerator is solved for the case of any general angular mode m. The ferrite is driven into saturation by a static magnetic field, resulting in the permeability tensor having off-diagonal elements. Expressions for the radial and angular transverse forces are obtained. Finally, we give numerical examples showing that the transverse forces in the anisotropic ferrite wake-field accelerator are reduced as the static saturated magnetization is increased.

I. INTRODUCTION

In a previous paper[1] (referred to here as I) we solved the theory of the anisotropic ferrite wake-field accelerator for the azimuthally symmetric $m=0$ mode. In that work it was shown that accelerating gradients of 1.5 [(MV/m)/nC] of driver beam charge are possible for realistic ferrite materials and that this number is comparable to that obtained for the dielectric wake-field accelerator. This is important since the next generation of wake-field acceleration experiments will have driver beam charges of 100 nC within bunch lengths of less than 10 psec traversing loaded waveguide structures.[2] The response of materials under such conditions is unknown at the present time; thus it is necessary to have several candidate materials available for loading the waveguides. Unmagnetized ferrites have been previously suggested by Callan *et al.*;[3] however, they conclude that the ferrite properties needed do not correspond to those of normal ferrites. On the other hand, in I we found that practically any magnetized ferrite will work.

In the present work we consider the case of the anisotropic ferrite wake-field accelerator for the case of any general angular mode m. This allows us to calculate the transverse forces arising from driver beam charges traveling off axis through the wake-field structure, as shown in Fig. 1. These unwanted transverse forces must be understood since they lead to beam instabilities. For smaller values of the ferrite static saturated magnetization, these transverse forces are about the same as those for the dielectric wake-field accelerator. But as the static saturated magnetization is increased, we find that these transverse forces are reduced in the ferrite-loaded structure. As in I, in this work we use mks units.

In I, we derived the ferrite permeability. Very briefly, the magnetic permeability and susceptibility tensors μ and χ are defined by

$$\mathbf{B}=\vec{\mu}\cdot\mathbf{H}\ , \tag{1}$$

with

$$\vec{\mu}=\mu_0(\vec{\mathrm{I}}+\vec{\chi})\equiv\mu_0\vec{\mu}_r \tag{2}$$

where $\vec{\mathrm{I}}$ is the identity matrix and $\vec{\mu}_r$ is the relative permeability and can be written

$$\vec{\mu}_r=\begin{bmatrix}\tilde{\mu}=1+\chi_{rr} & -iK & 0\\ iK & \tilde{\mu} & 0\\ 0 & 0 & \tilde{\mu}_z\end{bmatrix}\ . \tag{3}$$

Define

$$\chi_{rr}=\chi'-i\chi''\ , \tag{4}$$

$$K=K'-iK''\ , \tag{5}$$

$$\omega_m=-\Gamma_e M_s\ , \tag{6}$$

where χ_{rr} and K have been divided into real and imaginary parts, M_s is the saturated magnetization, and Γ_e is the gyromagnetic ratio which is given by

$$\Gamma_e=-g(\mu_0 e/2m_e)\ ,$$

with e and m_e being the charge and mass of the electron, μ_0 the permeability of free space, and g the spectroscopic splitting factor. Since $g=2$ for a free electron, in our case $\Gamma_e=-2.21\times10^5$ (rad/sec)/(At/m). The ferrite resonance frequency is $\omega_r=-\Gamma_e H_s$, where H_s is the dc magnetic field which drives the ferrite into saturation. With these definitions, the real and imaginary parts of the sus-

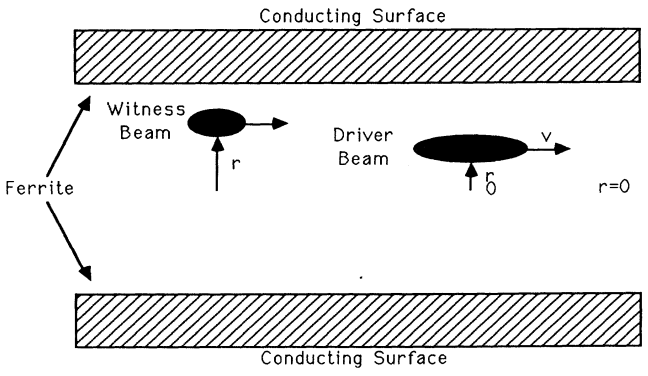

FIG. 1. Ferrite-loaded wake-field structure.

ceptibility tensor components become

$$\chi' = \frac{\omega_m \omega_r (\omega_r^2 - \omega^2) + \omega_m \omega_r \alpha^2 \omega^2}{[\omega_r^2 - \omega^2(1+\alpha^2)]^2 + 4\omega^2 \omega_r^2 \alpha^2} , \tag{7}$$

$$\chi'' = \frac{\omega_m \omega \alpha [\omega_r^2 + (1+\alpha^2)\omega^2]}{[\omega_r^2 - \omega^2(1+\alpha^2)]^2 + 4\omega^2 \omega_r^2 \alpha^2} , \tag{8}$$

$$K' = \frac{-\omega_m \omega [\omega_r^2 - \omega^2(1+\alpha^2)]}{[\omega_r^2 - \omega^2(1+\alpha^2)]^2 + 4\omega^2 \omega_r^2 \alpha^2} , \tag{9}$$

$$K'' = \frac{-2\omega_m \omega_r \omega^2 \alpha}{[\omega_r^2 - \omega^2(1+\alpha^2)]^2 + 4\omega^2 \omega_r^2 \alpha^2} , \tag{10}$$

where α is the damping constant. As in I, it has a small effect on our results so we can neglect it.

In the next section, we solve for the electromagnetic fields inside the ferrite and vacuum regions. In Sec. III we apply the boundary conditions and solve for the coefficients of the homogeneous electromagnetic field solutions. And finally, in Sec. IV we discuss the optimized anisotropic ferrite wake-field accelerator found in I but tuned to 20 Ghz and calculate its transverse forces.

II. FIELD SOLUTIONS

A. Vacuum hole region

As in I we consider the case where the driver is a line of charge having a Gaussian line distribution. But now it is located at the position $r = r_0$, $\theta = \theta_0 = 0$ and is given by

$$\rho(r,\theta,z-vt) = \frac{-Q}{\sqrt{2\pi}} \frac{\delta(r-r_0)}{r} \frac{\delta(\theta)}{\sigma_z} e^{-(z-vt)^2/2\sigma_z^2} \tag{11}$$

having the Fourier expansion

$$\rho(r,\theta,z-vt) = \frac{-Q}{(2\pi)^2} \frac{\delta(r-r_0)}{vr} \times \sum_{m=-\infty}^{\infty} e^{im\theta} \int_{-\infty}^{\infty} e^{-(i\omega/v)(z-vt)} \times e^{-\omega^2\sigma_z^2/2v^2} d\omega . \tag{12}$$

Fourier expansions for the longitudinal fields are taken to be

$$\begin{bmatrix} E_{mz}^h(r,\theta,z-vt) \\ H_{mz}^h(r,\theta,z-vt) \end{bmatrix} = \sum_{m=-\infty}^{\infty} \int_{-\infty}^{\infty} e^{im\theta} e^{-(i\omega/v)(z-vt)} \times \begin{bmatrix} E_{mz}^h(\omega,r) \\ H_{mz}^h(\omega,r) \end{bmatrix} d\omega . \tag{13}$$

Following I, we arrive at

$$E_{mz}^h(\omega,r) = \frac{-i\omega Q}{4\pi^2 \epsilon_0 v^2 \gamma^2} e^{-\omega^2\sigma_z^2/2v^2} I_m\left[\frac{\omega r_<}{v\gamma}\right] \times K_m\left[\frac{\omega r_>}{v\gamma}\right] + C_m I_m\left[\frac{\omega r}{v\gamma}\right] , \tag{14}$$

$$H_{mz}^h(\omega,r) = G_m I_m\left[\frac{\omega r}{v\gamma}\right] , \tag{15}$$

where I_m and K_m are the modified Bessel functions, γ is the Lorentz factor, and $r_<$ ($r_>$) means the lesser (greater) of r and r_0.

Solving for the transverse fields in terms of the longitudinal fields and specializing to the case $r_0 \le r$, we obtain

$$E_{mr}^h = i\gamma \left[\frac{-i\omega Q}{4\pi^2 \epsilon_0 v^2 \gamma^2} e^{-\omega^2\sigma_z^2/2v^2} I_m\left[\frac{\omega r_0}{v\gamma}\right] K_m'\left[\frac{\omega r}{v\gamma}\right] + C_m I_m'\left[\frac{\omega r}{v\gamma}\right] \right] e^{im\theta} e^{-(i\omega/v)(z-vt)} + \frac{i\mu_0 v^2\gamma^2}{\omega} \frac{im}{r} \left[G_m I_m\left[\frac{\omega r}{v\gamma}\right] \right] e^{im\theta} e^{-(i\omega/v)(z-vt)} , \tag{16}$$

$$E_{m\theta}^h = \frac{iv\gamma^2}{\omega} \frac{im}{r} \left[\frac{-i\omega Q}{4\pi^2 \epsilon_0 v^2 \gamma^2} e^{-\omega^2\sigma_z^2/2v^2} I_m\left[\frac{\omega r_0}{v\gamma}\right] K_m\left[\frac{\omega r}{v\gamma}\right] + C_m I_m\left[\frac{\omega r}{v\gamma}\right] \right] e^{im\theta} e^{-(i\omega/v)(z-vt)} - i\mu_0 v\gamma \left[G_m I_m'\left[\frac{\omega r}{v\gamma}\right] \right] e^{im\theta} e^{-(i\omega/v)(z-vt)} , \tag{17}$$

$$H_{mr}^h = \frac{-i\epsilon_0 v^2\gamma^2}{\omega} \frac{im}{r} \left[\frac{-i\omega Q}{4\pi^2 \epsilon_0 v^2 \gamma^2} e^{-\omega^2\sigma_z^2/2v^2} I_m\left[\frac{\omega r_0}{v\gamma}\right] K_m\left[\frac{\omega r}{v\gamma}\right] + C_m I_m\left[\frac{\omega r}{v\gamma}\right] \right] e^{im\theta} e^{-(i\omega/v)(z-vt)} + i\gamma \left[G_m I_m'\left[\frac{\omega r}{v\gamma}\right] \right] e^{im\theta} e^{-(i\omega/v)(z-vt)} , \tag{18}$$

$$H_{m\theta}^h = i\epsilon_0 v\gamma \left[\frac{-i\omega Q}{4\pi^2 \epsilon_0 v^2 \gamma^2} e^{-\omega^2\sigma_z^2/2v^2} I_m\left[\frac{\omega r_0}{v\gamma}\right] K_m'\left[\frac{\omega r}{v\gamma}\right] + C_m I_m'\left[\frac{\omega r}{v\gamma}\right] \right] e^{im\theta} e^{-(i\omega/v)(z-vt)} + \frac{iv\gamma^2}{\omega} \frac{im}{r} \left[G_m I_m\left[\frac{\omega r}{v\gamma}\right] \right] e^{im\theta} e^{-(i\omega/v)(z-vt)} . \tag{19}$$

C_m and G_m are constants to be determined in Sec. III by the boundary conditions.

B. Ferrite region

Assuming all fields vary as $e^{-\kappa z+i\omega t}$, the transverse electromagnetic field components can be written in terms of the longitudinal components as follows:

$$E^f_{mr}=p^f\frac{\partial E^f_{mz}}{\partial r}+q^f\frac{1}{r}\frac{\partial E^f_{mz}}{\partial\theta}+\bar{r}^f\frac{\partial H^f_{mz}}{\partial r}+s^f\frac{1}{r}\frac{\partial H^f_{mz}}{\partial\theta}\ , \tag{20}$$

$$E^f_{m\theta}=-q^f\frac{\partial E^f_{mz}}{\partial r}+p^f\frac{1}{r}\frac{\partial E^f_{mz}}{\partial\theta}-s^f\frac{\partial H^f_{mz}}{\partial r}+\bar{r}^f\frac{1}{r}\frac{\partial H^f_{mz}}{\partial\theta}\ , \tag{21}$$

$$H^f_{mr}=t^f\frac{\partial E^f_{mz}}{\partial r}+u^f\frac{1}{r}\frac{\partial E^f_{mz}}{\partial\theta}+p^f\frac{\partial H^f_{mz}}{\partial r}+q^f\frac{1}{r}\frac{\partial H^f_{mz}}{\partial\theta}\ , \tag{22}$$

$$H^f_{m\theta}=-u^f\frac{\partial E^f_{mz}}{\partial r}+t^f\frac{1}{r}\frac{\partial E^f_{mz}}{\partial\theta}-q^f\frac{\partial H^f_{mz}}{\partial r}+p^f\frac{1}{r}\frac{\partial H^f_{mz}}{\partial\theta}\ , \tag{23}$$

where

$$p^f=-\kappa(\kappa^2+\omega^2\epsilon_f\mu_0\tilde{\mu})(\Delta^f)^{-1}\ , \tag{24}$$

$$q^f=-i\kappa\omega^2\epsilon_f\mu_0K(\Delta^f)^{-1}\ , \tag{25}$$

$$\bar{r}^f=\omega\mu_0K\kappa^2(\Delta^f)^{-1}\ , \tag{26}$$

$$s^f=-i\omega[\mu_0\tilde{\mu}\kappa^2+\omega^2\mu_0^2(\tilde{\mu}^2-K^2)\epsilon_f](\Delta^f)^{-1}\ , \tag{27}$$

$$t^f=\omega^3\epsilon_f^2\mu_0K(\Delta^f)^{-1}\ , \tag{28}$$

$$u^f=i\omega(\epsilon_f\kappa^2+\omega^2\epsilon_f^2\mu_0\tilde{\mu})(\Delta^f)^{-1}\ , \tag{29}$$

$$\Delta^f=[\kappa^2+\omega^2\epsilon_f\mu_0(\tilde{\mu}+K)][\kappa^2+\omega^2\epsilon_f\mu_0(\tilde{\mu}-K)]\ . \tag{30}$$

We will only require boundary conditions for E^f_{mz}, H^f_{mz}, $E^f_{m\theta}$, and $H^f_{m\theta}$. Thus, carrying out a program similar to that in I, we arrive at the following field solutions inside the ferrite for any general mode m:

$$E^f_{mz}=[A_{m1}J_m(k_1r)+B_{m1}N_m(k_1r)+A_{m2}J_m(k_2r)+B_{m2}N_m(k_2r)]e^{im\theta}e^{-\kappa z+i\omega t}\ , \tag{31}$$

$$H^f_{mz}=\frac{\tilde{\mu}}{\kappa\omega\mu_0\tilde{\mu}_zK}\left[\left[k_1^2-\kappa^2-\omega^2\epsilon_f\mu_0\frac{\tilde{\mu}^2-K^2}{\tilde{\mu}}\right][A_{m1}J_m(k_1r)+B_{m1}N_m(k_1r)]+\left[k_2^2-\kappa^2-\omega^2\epsilon_f\mu_0\frac{\tilde{\mu}^2-K^2}{\tilde{\mu}}\right][A_{m2}J_m(k_2r)+B_{m2}N_m(k_2r)]\right]e^{im\theta}e^{-\kappa z+i\omega t}\ , \tag{32}$$

$$\begin{aligned}E^f_{m\theta}=&\,i\kappa\omega^2\epsilon_f\mu_0K(\Delta^f)^{-1}\{k_1[A_{m1}J'_m(k_1r)+B_{m1}N'_m(k_1r)]+k_2[A_{m2}J'_m(k_2r)+B_{m2}N'_m(k_2r)]\}e^{im\theta}e^{-\kappa z+i\omega t}\\&-\kappa(\kappa^2+\omega^2\epsilon_f\mu_0\tilde{\mu})(\Delta^f)^{-1}\left[\frac{im}{r}\right][A_{m1}J_m(k_1r)+B_{m1}N_m(k_1r)+A_{m2}J_m(k_2r)+B_{m2}N_m(k_2r)]e^{im\theta}e^{-\kappa z+i\omega t}\\&+i[\tilde{\mu}\kappa^2+\omega^2\mu_0(\tilde{\mu}^2-K^2)\epsilon_f](\Delta^f)^{-1}\frac{\tilde{\mu}}{\kappa\tilde{\mu}_zK}\\&\times\left[\left[k_1^2-\kappa^2-\omega^2\epsilon_f\mu_0\frac{\tilde{\mu}^2-K^2}{\tilde{\mu}}\right]\{k_1[A_{m1}J'_m(k_1r)+B_{m1}N'_m(k_1r)]\}+\left[k_2^2-\kappa^2-\omega^2\epsilon_f\mu_0\frac{\tilde{\mu}^2-K^2}{\tilde{\mu}}\right]\{k_2[A_{m2}J'_m(k_2r)+B_{m2}N'_m(k_2r)]\}\right]e^{im\theta}e^{-\kappa z+i\omega t}\\&+\kappa(\Delta^f)^{-1}\left[\frac{im}{r}\right]\frac{\tilde{\mu}}{\tilde{\mu}_z}\left[\left[k_1^2-\kappa^2-\omega^2\epsilon_f\mu_0\frac{\tilde{\mu}^2-K^2}{\tilde{\mu}}\right][A_{m1}J_m(k_1r)+B_{m1}N_m(k_1r)]+\left[k_2^2-\kappa^2-\omega^2\epsilon_f\mu_0\frac{\tilde{\mu}^2-K^2}{\tilde{\mu}}\right][A_{m2}J_m(k_2r)+B_{m2}N_m(k_2r)]\right]e^{im\theta}e^{-\kappa z+i\omega t}\ ,\end{aligned} \tag{33}$$

$$
\begin{aligned}
H^f_{m\theta} = &-i\omega(\epsilon_f\kappa^2+\omega^2\epsilon_f^2\mu_0\tilde{\mu})(\Delta^f)^{-1}\{k_1[A_{m1}J'_m(k_1r)+B_{m1}N'_m(k_1r)] \\
&\qquad +k_2[A_{m2}J'_m(k_2r)+B_{m2}N'_m(k_2r)]\}e^{im\theta}e^{-\kappa z+i\omega t} \\
&+\omega^3\epsilon_f^2\mu_0K(\Delta^f)^{-1}\left[\frac{im}{r}\right][A_{m1}J_m(k_1r)+B_{m1}N_m(k_1r)+A_{m2}J_m(k_2r)+B_{m2}N_m(k_2r)]e^{im\theta}e^{-\kappa z+i\omega t} \\
&+i\omega\epsilon_f(\Delta_f)^{-1}\frac{\tilde{\mu}}{\tilde{\mu}_z}\left[\left[k_1^2-\kappa^2-\omega^2\epsilon_f\mu_0\frac{\tilde{\mu}^2-K^2}{\tilde{\mu}}\right]\{k_1[A_{m1}J'_m(k_1r)+B_{m1}N'_m(k_1r)]\}\right. \\
&\qquad \left.+\left[k_2^2-\kappa^2-\omega^2\epsilon_f\mu_0\frac{\tilde{\mu}^2-K^2}{\tilde{\mu}}\right]\{k_2[A_{m2}J'_m(k_2r)+B_{m2}N'_m(k_2r)]\}\right] \\
&\times e^{im\theta}e^{-\kappa z+i\omega t}-(\kappa^2+\omega^2\epsilon_f\mu_0\tilde{\mu})(\Delta^f)^{-1}\left[\frac{im}{r}\right]\frac{\tilde{\mu}}{\omega\mu_0\tilde{\mu}_zK} \\
&\times\left[\left[k_1^2-\kappa^2-\omega^2\epsilon_f\mu_0\frac{\tilde{\mu}^2-K^2}{\tilde{\mu}}\right][A_{m1}J_m(k_1r)+B_{m1}N_m(k_1r)]\right. \\
&\qquad \left.+\left[k_2^2-\kappa^2-\omega^2\epsilon_f\mu_0\frac{\tilde{\mu}^2-K^2}{\tilde{\mu}}\right][A_{m2}J_m(k_2r)+B_{m2}N_m(k_2r)]\right]e^{im\theta}e^{-\kappa z+i\omega t}\,,
\end{aligned}
\tag{34}
$$

where J_m and N_m are mth-order Bessel functions, A_{m1}, A_{m2}, B_{m1}, and B_{m2} are constants to be determined by boundary conditions, and

$$
\begin{aligned}
k^2_{1,2} = &\tfrac{1}{2}\left[\kappa^2\left[1+\frac{\tilde{\mu}_z}{\tilde{\mu}}\right]+\omega^2\mu_0\epsilon_f\frac{\tilde{\mu}^2-K^2}{\tilde{\mu}}+\omega^2\epsilon_f\mu_0\tilde{\mu}_z\right] \\
&\pm\tfrac{1}{2}\left\{\left[\kappa^2\left[1-\frac{\tilde{\mu}_z}{\tilde{\mu}}\right]+\omega^2\mu_0\epsilon_f\frac{\tilde{\mu}^2-K^2}{\tilde{\mu}}-\omega^2\epsilon_f\mu_0\tilde{\mu}_z\right]^2-4\kappa^2\omega^2\epsilon_f\mu_0\tilde{\mu}_z\left[\frac{K}{\tilde{\mu}}\right]^2\right\}^{1/2}\,.
\end{aligned}
\tag{35}
$$

III. BOUNDARY CONDITIONS

We choose the following boundary conditions:

$$E^f_{mz}(r=b)=0\,, \tag{36}$$

$$E^f_{mz}(r=a)=E^h_{mz}(r=a)\,, \tag{37}$$

$$H^f_{mz}(r=a)=H^h_{mz}(r=a)\,, \tag{38}$$

$$E^f_{m\theta}(r=a)=E^h_{m\theta}(r=a)\,, \tag{39}$$

$$H^f_{m\theta}(r=a)=H^h_{m\theta}(r=a)\,, \tag{40}$$

$$E^f_{m\theta}(r=b)=0\,. \tag{41}$$

Also, to match the arguments of the exponentials from the ferrite and vacuum regions we must have $\kappa=i\omega/v$ so that from Eq. (35) we get

$$
\begin{aligned}
k^2_{1,2} = &\frac{\omega^2}{2}\left[-\frac{1}{v^2}\left[1+\frac{\tilde{\mu}_z}{\tilde{\mu}}\right]+\mu_0\epsilon_f\frac{\tilde{\mu}^2-K^2}{\tilde{\mu}}+\epsilon_f\mu_0\tilde{\mu}_z\right] \\
&\pm\frac{\omega^2}{2}\left\{\left[-\frac{1}{v^2}\left[1-\frac{\tilde{\mu}_z}{\tilde{\mu}}\right]+\mu_0\epsilon_f\frac{\tilde{\mu}^2-K^2}{\tilde{\mu}}-\epsilon_f\mu_0\tilde{\mu}_z\right]^2+4\frac{\epsilon_f}{v^2}\mu_0\tilde{\mu}_z\left[\frac{K}{\tilde{\mu}}\right]^2\right\}^{1/2}\,.
\end{aligned}
\tag{42}
$$

The boundary conditions can be cast in the form

$$M_m X_m = Y_m \ , \tag{43}$$

where

$$M_m = \begin{bmatrix} \alpha_{m1} & \beta_{m1} & \delta_{m1} & \gamma_{m1} & 0 & 0 \\ \alpha_{m2} & \beta_{m2} & \delta_{m2} & \gamma_{m2} & \nu_{m2} & 0 \\ \alpha_{m3} & \beta_{m3} & \delta_{m3} & \gamma_{m3} & 0 & \lambda_{m3} \\ \alpha_{m4} & \beta_{m4} & \delta_{m4} & \gamma_{m4} & \nu_{m4} & \lambda_{m4} \\ \alpha_{m5} & \beta_{m5} & \delta_{m5} & \gamma_{m5} & \nu_{m5} & \lambda_{m5} \\ \alpha_{m6} & \beta_{m6} & \delta_{m6} & \gamma_{m6} & 0 & 0 \end{bmatrix} , \tag{44}$$

$$X_m = \begin{bmatrix} A_{m1} \\ B_{m1} \\ A_{m2} \\ B_{m2} \\ C_m \\ G_m \end{bmatrix}, \quad Y_m = \begin{bmatrix} 0 \\ d_{m2} \\ 0 \\ d_{m4} \\ d_{m5} \\ 0 \end{bmatrix} . \tag{45}$$

The excitation frequencies are determined by the zeros of the determinant of the matrix M_m. Only C_m is needed for the accelerating wake field E^h_{mz}, and we have

$$C_m = \frac{\det M_m(\nu_{mi} \to d_{mi})}{\det M_m} \ , \tag{46}$$

where in the numerator we mean to replace the coefficients ν_{mi} by the quantities d_{mi}. Thus, for the accelerating wake field, we obtain

$$E^h_{mz}(r,\theta,z-vt) = \sum_{m=-\infty}^{\infty} \int_{-\infty}^{\infty} e^{im\theta} e^{-(i\omega/v)(z-vt)} \left[\frac{\det M_m(\nu_{mi} \to d_{mi})}{\det M_m} I_m\left[\frac{\omega r}{v\gamma}\right] - \frac{iQ\omega}{4\pi^2\epsilon_0 v^2\gamma^2} e^{-\omega^2\sigma_z^2/2v^2} I_m\left[\frac{\omega r_0}{v\gamma}\right] K_m\left[\frac{\omega r}{v\gamma}\right] \right] d\omega \ . \tag{47}$$

In the next section we consider numerical examples.

IV. DISCUSSION AND CONCLUSIONS

We consider the following optimized list of parameters for a lowest $m=0$ frequency pole of 20 Ghz:

rms length of driver bunch $\sigma_z = 0.7$ mm , (48)

energy of driver bunch $= 150$ MeV ($\beta = 0.999\,994$) , (49)

inner ferrite radius $a = 3$ mm , (50)

outer ferrite radius $b = 4.2$ mm , (51)

$M_s = 10^5$ At/m , (52)

$H_s = 2.0 \times 10^3$ At/m , (53)

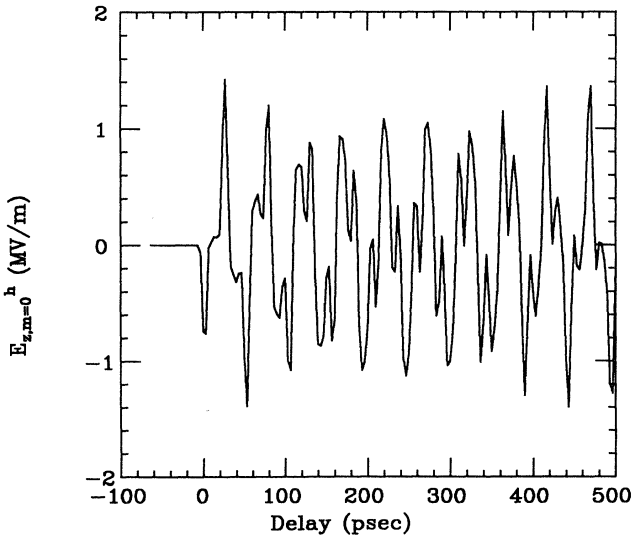

FIG. 2. Accelerating wake field $E^h_{z,m=0}$ vs delay (distance) behind the driver beam for the optimized ferrite structure: $a=3$ mm, $b=4.2$ mm, $Q=1$ nC, $\beta=0.999\,994$, $\sigma_z=0.7$ mm, $M_s=10^5$ At/m, $H_s=2\times10^3$ At/m, $\epsilon_f=10\epsilon_0$. $r=r_0=0$.

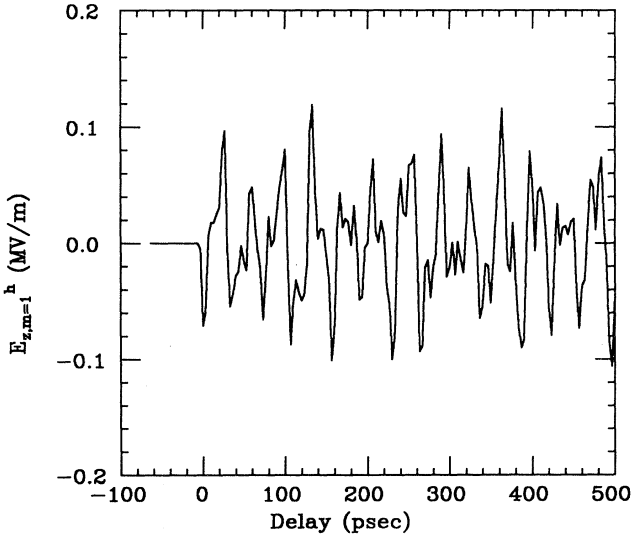

FIG. 3. Accelerating wake field $E^h_{z,m=1}$ vs delay (distance) behind the driver beam for the optimized ferrite structure: $a=3$ mm, $b=4.2$ mm, $Q=1$ nC, $\beta=0.999\,994$, $\sigma_z=0.7$ mm, $M_s=10^5$ At/m, $H_s=2\times10^3$ At/m, $\epsilon_f=10\epsilon_0$. $r=r_0=1.0$ mm.

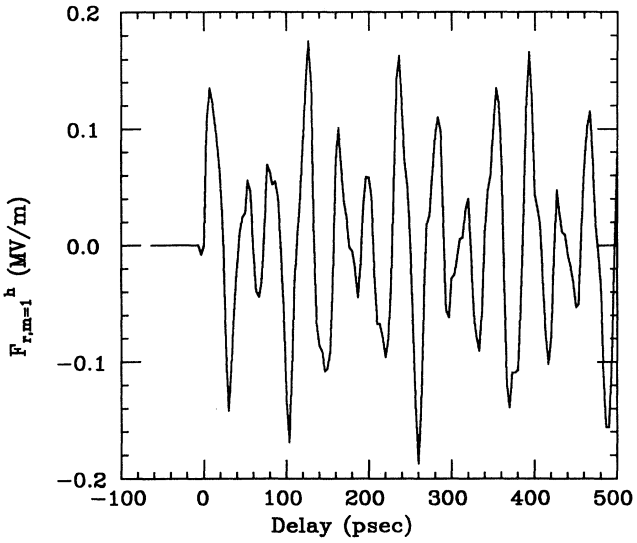

FIG. 4. Radial force per unit electron test (witness beam) charge $F^h_{r,m=1}$ vs delay (distance) behind the driver beam for the optimized ferrite structure: $a=3$ mm, $b=4.2$ mm, $Q=1$ nC, $\beta=0.999\,994$, $\sigma_z=0.7$ mm, $M_s=10^5$ At/m, $H_s=2\times10^3$ At/m, $\epsilon_f=10\epsilon_0$. $r=r_0=1.0$ mm.

$$\epsilon_f=10\epsilon_0\ , \tag{54}$$

$$\tilde{\mu}_z=1.0\ . \tag{55}$$

For $m=0$ and 1, graphs of E^h_{mz} versus delay behind the driver are shown in Figs. 2 and 3.

The Fourier transforms of the transverse forces per unit electron test (witness beam) charge behind the driver are related to the transforms of the longitudinal wake

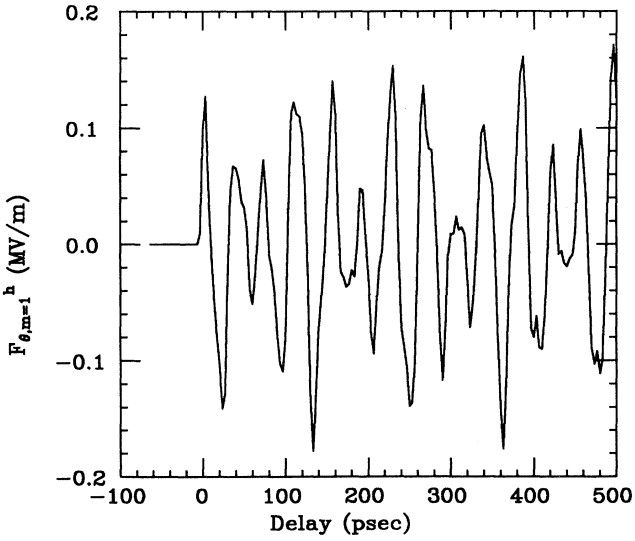

FIG. 5. Angular force per unit electron test charge $F^h_{\theta,m=1}$ vs delay (distance) behind the driver beam for the optimized ferrite structure: $a=3$ mm, $b=4.2$ mm, $Q=1$ nC, $\beta=0.999\,994$, $\sigma_z=0.7$ mm, $M_s=10^5$ At/m, $H_s=2\times10^3$ At/m, $\epsilon_f=10\epsilon_0$. $r=r_0=1.0$ mm.

TABLE I. Maximum $m=1$ mode radial force $F_r^{h,\max}$ (per test charge e and per nC of driver charge) and the two lowest-frequency pole contributions f_1 and f_2 vs applied static magnetic field H_s for $M_s=10^5$ At/m ($B_s=4\pi M_s=1257$ G in cgs units), $a=3$ mm, $b=4.2$ mm, $\epsilon_f=10\epsilon_0$, $r=r_0=1$ mm.

H_s (At/m)	f_1 (GHz)	f_2 (GHz)	$F_r^{h,\max}$ [(MV/m)/nC]
5×10^2	18.08	26.10	0.136
10^3	18.08	26.10	0.135
2×10^3	18.08	26.10	0.135
3×10^3	18.08	26.10	0.135
4×10^3	18.08	26.11	0.135

TABLE II. Maximum $m=1$ mode radial force $F_r^{h,\max}$ (per test charge e and per nC of driver charge) and the two lowest-frequency pole contributions f_1 and f_2 vs saturated static magnetization M_s for $H_s=2\times10^3$ At/m ($H_s=25$ Oe in cgs units), $a=3$ mm, $b=4.2$ mm, $\epsilon_f=10\epsilon_0$, $r=r_0=1$ mm.

M_s (At/m)	f_1 (GHz)	f_2 (GHz)	$F_r^{h,\max}$ [(MV/m)/nC]
10^4	18.90	25.51	0.140
10^5	18.08	26.10	0.135
2×10^5	17.74	27.05	0.117
3×10^5	17.74	28.34	0.0991
4×10^5	17.91	29.97	0.0826
5×10^5	18.17	31.95	0.0741
6×10^5	18.38	34.25	0.0667

TABLE III. Maximum $m=1$ mode angular force $F_\theta^{h,\max}$ (per test charge e and per nC of driver charge) and the two lowest-frequency pole contributions f_1 and f_2 vs applied static magnetic H_s for $M_s=10^5$ At/m ($B_s=4\pi M_s=1257$ G in cgs units), $a=3$ mm, $b=4.2$ mm, $\epsilon_f=10\epsilon_0$, $r=r_0=1$ mm.

H_s (At/m)	f_1 (GHz)	f_2 (GHz)	$F_\theta^{h,\max}$ [(MV/m)/nC]
5×10^2	18.08	26.10	0.127
10^3	18.08	26.10	0.127
2×10^3	18.08	26.10	0.127
3×10^3	18.08	26.10	0.126
4×10^3	18.08	26.11	0.126

TABLE IV. Maximum $m=1$ mode angular force $F_\theta^{h,\max}$ (per test charge e and per nC of driver charge) and the two lowest-frequency pole contributions f_1 and f_2 vs saturated static magnetization M_s for $H_s=2\times10^3$ At/m ($H_s=25$ Oe in cgs units), $a=3$ mm, $b=4.2$ mm, $\epsilon_f=10\epsilon_0$, $r=r_0=1$ mm.

M_s (At/m)	f_1 (GHz)	f_2 (GHz)	$F_\theta^{h,\max}$ [(MV/m)/nC]
10^4	18.90	25.51	0.130
10^5	18.08	26.10	0.127
2×10^5	17.74	27.05	0.105
3×10^5	17.74	28.34	0.0829
4×10^5	17.91	29.97	0.0637
5×10^5	18.17	31.95	0.0533
6×10^5	18.38	34.25	0.0451

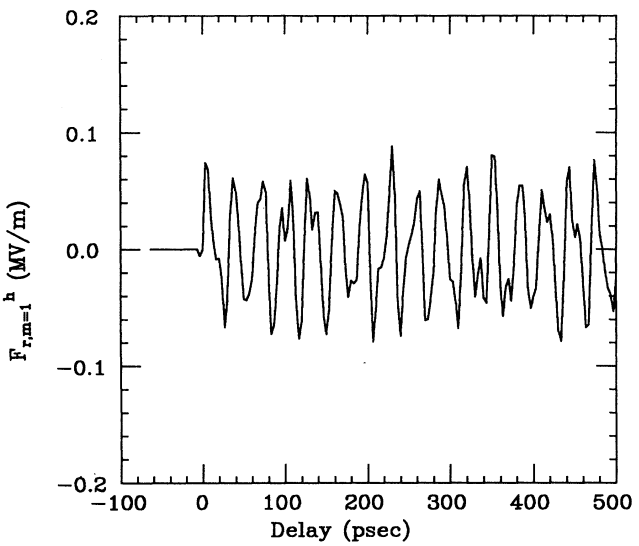

FIG. 6. Radial force per unit electron test charge $F^h_{r,m=1}$ vs delay (distance) behind the driver beam for $a=3$ mm, $b=4.2$ mm, $Q=1$ nC, $\beta=0.999\,994$, $\sigma_z=0.7$ mm, $M_s=5\times10^5$ At/m, $H_s=2\times10^3$ At/m, $\epsilon_f=10\epsilon_0$, $r=r_0=1.0$ mm.

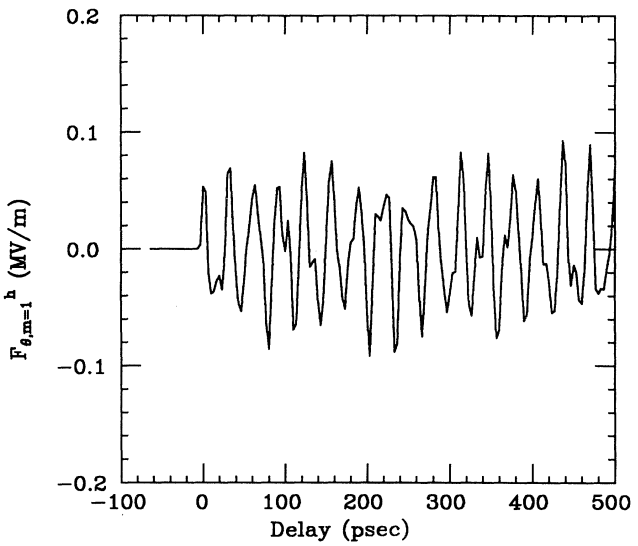

FIG. 7. Angular force per unit electron test charge $F^h_{\theta,m=1}$ vs delay (distance) behind the driver beam for $a=3$ mm, $b=4.2$ mm, $Q=1$ nC, $\beta=0.999\,994$, $\sigma_z=0.7$ mm, $M_s=5\times10^5$ At/m, $H_s=2\times10^3$ At/m, $\epsilon_f=10\epsilon_0$, $r=r_0=1.0$ mm.

field by the Panofsky-Wenzel theorem:[4]

$$F^h_{mr}=\frac{iv}{\omega}\frac{\partial E^h_{mz}}{\partial r}\ , \tag{56}$$

$$F^h_{m\theta}=-\frac{mv}{\omega r}E^h_{mz}\ . \tag{57}$$

Graphs of the transverse forces per unit electron test charge for the $m=1$ mode are given in Figs. 4 and 5.

It is now known how to damp transverse forces at the position of the trailing witness beam pulse behind the driver.[5] However, one is still confronted by the beam breakup instabilities for the driver beam itself. To consider this point, in Tables I–IV we display the numerical evaluations of the $m=1$ mode maximum transverse forces inside the driver beam (out to 6.7 psec behind the center of the driver and in units of [(MV/m)/nC] of driver charge) and the two lowest-frequency pole contributions versus applied static magnetic field H_s and saturated static magnetization M_s.

We find that the transverse forces and excitation frequencies are not sensitive to H_s. However, we see a clear reduction of the transverse forces as M_s increases. In Figs. 6 and 7 we show graphs of the transverse forces versus delay behind the driver for $M_s=5\times10^5$. They are to be compared with Figs. 4 and 5 where $M_s=10^5$. Since we found in I that the longitudinal acceleration gradient is not very sensitive to M_s, this work shows that we can reduce transverse forces by increasing M_s without decreasing the acceleration gradient very much. Thus, for the anisotropic wake-field accelerator, the beam breakup problems are not as severe as in other wake-field acceleration schemes.

For comparison, the 20-GHz dielectric wake-field structure,[6–9] with optimal $\epsilon_d=3\epsilon_0$, has been investigated. There we find that the maximum radial and angular $m=1$ mode forces inside the driver beam at $r=r_0=1$ mm are 0.141 and 0.115 [(MV/m)/nC] of driver charge, respectively, and the two lowest-frequency pole contributions are 17.08 and 29.93 Ghz.

To conclude, we have solved the theory for the anisotropic ferrite wake-field accelerator for any mode m. Further, we have given some numerical examples and compared the results to the dielectric wake-field accelerator. We find that in the anisotropic ferrite wake-field accelerator, the acceleration gradient is slightly less; however, the transverse forces can be reduced by increasing the saturation magnetization so that the beam breakup problems are not as bad as that of the dielectric accelerator.

ACKNOWLEDGMENTS

The authors would like to thank W. Gai and M. Rosing for many helpful discussions. This work was supported by the U.S. Department of Energy under Contract No. W-31-109-ENG-38. One of us (J.C.) would like to thank Argonne National Laboratory's Division of Educational Programs for support.

[1]S. Mtingwa, preceding paper, Phys. Rev. A **43**, 5581 (1991).
[2]J. Simpson *et al.* (unpublished).
[3]C. Callan *et al.* (unpublished).
[4]W. K. H. Panofsky and W. A. Wenzel, Rev. Sci. Instrum. **27**, 967 (1956).
[5]E. Chojnacki, J. Appl. Phys. (to be published).
[6]M. Jones, R. Keinigs, and W. Peter, Los Alamos Report No. LUR-89-4234 (unpublished).
[7]M. Rosing and W. Gai, Phys. Rev. D **42**, 1829 (1990).
[8]K. Ng, Phys. Rev. D **42**, 1819 (1990).
[9]R. Gluckstern (private communication).